PHILOSOPHICAL TRANSACTIONS OF THE ROYAL SOCIETY A MATHEMATICAL, PHYSICAL & ENGINEERING SCIENCES

Improvements in High Temperature Oxidation Resistance by Additions of Reactive Elements or Oxide Dispersions

D. P. Whittle and J. Stringer

Phil. Trans. R. Soc. Lond. A 1980 **295**, 309-329
doi: 10.1098/rsta.1980.0124

Phil. Trans. R. Soc. Lond. A **295**, 309–329 (1980) [309]
Printed in Great Britain

VIII. IMPROVEMENT IN PROPERTIES: ADDITIVES IN OXIDATION RESISTANCE

Improvements in high temperature oxidation resistance by additions of reactive elements or oxide dispersions

By D. P. Whittle†§ and J. Stringer‡

† *Department of Metallurgy and Materials Science, University of Liverpool, P.O. Box* 147, *Liverpool L*69 3*BX, U.K.*

‡ *Electric Power Research Institute, Palo Alto, California, U.S.A.*

[Plates 1 and 2]

The improvement in oxidation resistance of high temperature alloys as a result of additions of rare earth elements, other reactive metals, or dispersions of stable oxides, has been known for many years. Two effects seem the most important: first, the adhesion between scale and alloy is markedly improved and this increases the alloy's resistance to thermal cycling exposure; secondly, in some but not all cases the actual growth rate of the oxide is also reduced. The various models proposed to explain these phenomena are discussed in the light of currently available experimental evidence. The most significant of these involve modification to the early, transient stages of oxidation, doping of the oxide which changes its transport properties, mechanical keying of the surface scale to the substrate by the formation of intrusions of oxide penetrating into the alloy and the elimination of void formation at the alloy–scale interface. The efficacies of the various beneficial additions are compared.

1. Introduction

There are two essential requirements for alloys which are designed to withstand degradation by oxidation during high temperature exposure. First, they must form a surface oxide which thickens only at a slow rate, and secondly this oxide layer must remain adherent to the alloy surface under all conditions. Cr_2O_3 and Al_2O_3 are generally regarded as the best protective oxides: diffusion through them is relatively slow in comparison with most other oxides, and since they are also stable, relatively little difficulty exists in selecting an alloy which contains sufficient chromium or aluminium to provide, by selective oxidation, a protective Cr_2O_3 or Al_2O_3 scale under various service environments. Cr_2O_3-forming alloys generally contain less than 2–3 % Al (unless otherwise indicated, all compositions are in percentages by mass) and 15 % Cr or more depending on the alloy base. Al_2O_3-forming alloys, on the other hand, in addition to at least 5 % Al usually also contain substantial amounts of chromium.

Even though an alloy contains sufficient chromium or aluminium to develop the appropriate protective oxide, this usually does not occur immediately on exposure to an oxidizing atmosphere. When oxygen is admitted to a clean alloy surface at elevated temperatures, nuclei of all possible oxides are formed, and the amounts of these oxides are such that the proportion of metal atoms is essentially the same as that of the surface of the alloy. The different nuclei

§ Present address: Lawrence Berkeley Laboratory, University of California, Berkeley, California 94720, U.S.A.

grow laterally, covering the surface at rates which cannot be predicted. In addition, they grow outwards and the base metal oxides tend to outgrow the protective oxide, Cr_2O_3 or Al_2O_3. However, because of its greater stability, the protective oxide will continue to grow laterally, until eventually the alloy surface is covered with a continuous layer of this oxide. At this point, growth of the base metal oxides will to all intents and purposes cease, and thereafter the overall oxidation rate is controlled by the growth of the protective oxide layer. This initial development of a continuous protective oxide layer has been termed the transient stage of oxidation (Whittle & Wood 1968); its duration depends on a number of factors including alloy composition, surface finish and the conditions of initial exposure of the material to the oxidizing environment, as discussed by Wood (1971).

The second requirement is that of adhesion, since during exposure environmental changes or stresses accompanying scale growth can cause loss of adhesion and spallation of the oxide. Numerous factors may affect oxide adhesion, but if consideration of mechanical disturbance is neglected, probably that of most importance is thermal cycling. During heating or cooling, stresses are developed owing to differences in thermal expansion or contraction of the oxide and alloy and these lead to spallation of the protective oxide and excessive rates of metal loss.

Empirically, it was discovered over 40 years ago that additions of rare earth metals as a melt deoxidant to Nichrome (Ni–20 %Cr) heating elements produced substantial increases in their lifetimes to failure in cyclic heating and cooling tests (Pfeil 1937): the protective oxide was more adherent. Yttrium and scandium additions were included in the original patent, and it was also shown that by the combined addition of rare earths, alkaline earths and carbon, the life of heat resisting alloys could be further improved. The amounts of the additions were such that 0.01–0.5 % rare earth, about 0.001–0.05 % Ca and up to about 0.25 % C remained in the finished alloy. A subsequent patent (Pfeil 1945) indicated that surface coatings of the same elements, their oxides, hydroxides or other salts that would decompose to oxides at high temperature could provide an alternative to alloy additions in improving oxidation resistance. The improvement effected by coating was not always as great as when the additive was included in the alloy, but this was more than compensated for by there being no detrimental effects to creep resistance. Surface coatings were applied either by dipping in a solution of the salt, or anodically. This 'rare earth effect', as it became known, was not confined to rare earth element additions. Pfeil (1945) in fact, indicated that elements from Groups II, III, IV and V of the Periodic Table could be used although their effectiveness decreased on passing from Group II to Group V, but increased with increasing atomic mass within a particular group.

As will be seen in § 2, subsequent work has confirmed that a wide range of additions can have a similar effect. Indeed, fine distributions of stable oxides in the alloy are perhaps even more effective in improving an alloy's performance under thermal cycling conditions. In many cases the two effects are indistinguishable, and may indeed be identical.

Improvement in scale adhesion is not the only beneficial effect, although it is usually the most dramatic (§ 6). The initial development of the protective oxide may also be modified (§ 4) with additions generally promoting the selective oxidation of chromium or aluminium from the alloy. The growth rate of the scale may also be reduced (§ 5), although it is often difficult to distinguish from this the effects related to increased scale–alloy adhesion.

This review, then, sets out to examine the various effects that minor additions of reactive elements or stable oxides have on the oxidation behaviour of high temperature alloys and the various mechanisms put forward to explain these effects.

PHILOSOPHICAL TRANSACTIONS OF THE ROYAL SOCIETY A MATHEMATICAL, PHYSICAL & ENGINEERING SCIENCES

2. Experimental observations

(a) *Chromia-forming alloys*

In Fe–Cr base alloys, early workers demonstrated that additions of Y to 25Cr–20Ni–Nb austenitic steels improved the overall oxidation resistance in CO_2 in the temperature range 800–1200 °C (Francis & Whitlow 1966; Antill & Peakall 1967). Generally, the effect seemed to be independent of the content of Y, and greatest at temperatures of 1000 °C and above; in all cases the adherence of the oxide scale was markedly improved, but there may also have been a reduction in growth rate of the oxide. Antill *et al.* (1976) found that similar effects could be produced by ion implantation of Y or Ce to a concentration of 0.2–0.8 % at a depth of 0.2 μm below the metal surface. Improvements in oxidation resistance of a 20Cr–25Ni–Nb steel persisted for periods of 4000–5000 h at 800 and 850 °C in CO_2, in spite of the fact that the layer of addition would have been oxidized after a maximum of 500 and 150 h at these two temperatures respectively.

Francis & Whitlow (1965) suggest that while the oxidation rate of an Fe–25Cr alloy is approximately parabolic, that of an Fe–25Cr–1Y alloy is asymptotic, and after an initially fast rate of attack slows down very rapidly. Wood & Boustead (1968) indicate similar behaviour for Gd and Y additions to Fe–27Cr alloys. However, Y was not able to prevent breakaway attack in Fe–16Cr alloys at 1200 °C, or during thermal cycling (Wright & Wilcox 1974); Zr (Wright & Wilcox 1974) and Gd (Wood & Boustead 1968), however, tended to increase the time to breakaway. A 3 % (by volume) addition of Y_2O_3 as a fine oxide dispersion was more effective, and rapid breakaway oxidation of Fe–16Cr at 1100 °C was never observed (Wright & Wilcox 1974). Goncel *et al.* (1979) have studied the effects of TiO_2, HfO_2 and TiN dispersions on the oxidation behaviour of both ferritic and austenitic stainless steels. Each addition reduced the overall oxidation rate but the oxide dispersions were generally much better than the nitride, and HfO_2 better than TiO_2.

In Co–30Cr, a 0.1Y addition significantly reduced the oxidation kinetics of Cr_2O_3 growth to 'cubic' rate behaviour instead of the parabolic-type behaviour observed with the binary alloy (Beltran 1970). In addition, scale adherence was improved up to 1100 °C, and there were no nodular growths of spinel and CoO as observed in the binary alloy. On the other hand, 1 % additions of Ti, Zr or Hf had no effect on the oxidation behaviour of Co–15Cr in the temperature range 1000–1200 °C (Whittle *et al.* 1977) and the scales produced were characteristic of the chromium content of the binary alloy: an outer layer of CoO and an inner layer containing the spinel, $CoCr_2O_4$, and particles of Cr_2O_3; no continuous layer of Cr_2O_3 developed. If, on the other hand, the reactive element addition was first converted to an oxide dispersion, subsequent oxidation produced a continuous, well adhered protective Cr_2O_3 layer, with very little Co-containing oxides. This conversion of the reactive element to an internal oxide dispersion was achieved by a treatment in a sealed pack in which the oxygen activity was sufficiently low to oxidize only the reactive element and not the chromium or cobalt. Thus, in terms of promoting selective oxidation of chromium, an oxide dispersion is clearly more effective than the corresponding active metal addition. Stringer & Wright (1972) showed that dispersed oxide containing Co–Cr alloys produced by more conventional means, attritor milling and powder compaction, also behaved in a similar way: a Co–21Cr–3 %Y_2O_3 (by volume) alloy developed Cr_2O_3 as a protective oxide, whereas a binary alloy of this composition would not (Kofstad & Hed 1970). Indeed, the growth rate of the Cr_2O_3 on the dispersion-containing alloy was considerably less

than that of Cr_2O_3 on a Co–35Cr alloy at 1200 °C; the differences were not so great at 900 °C.

Following the early work on additions to Nichrome heating elements referred to in § 1, there has been surprisingly little effort on metallic additions to Ni–Cr alloys. Strafford & Harrison (1976) made additions of 0.5Y, La, Ce, Sm, Th, U, Zr or V to Ni–15Cr: La, Ce and Th produced progressively enhanced rates of oxidation relative to the binary alloy at 900 °C, whereas Y, Sm, V, U and Zr effected increasingly reduced rates of oxidation in the order given. None of the alloys, however, developed truly protective scales of Cr_2O_3. Equally, although Zr, Hf, La, Ce, Sm or Er increased the oxidation resistance of a Ni–10Cr alloy during both isothermal and thermal cycling tests at 1000–1200 °C, the alloy chromium content was too low for a continuous Cr_2O_3 scale (Ryabkina & Rogel'berg 1976). Similar additions to a Ni–10Cr–1.8Si alloy produced no effect in isothermal conditions, but increased the resistance under thermal cycling conditions: formation of a protective layer of SiO_2 in the scale was encouraged.

Ni–Cr alloys containing dispersed oxides have been studied in much more detail. These include Y_2O_3 (Stringer *et al.* 1972*b*; Wright *et al.* 1975; Michels 1976), La_2O_3 (Michels 1976), Al_2O_3 (Wright *et al.* 1975; Michels 1976), Li_2O (Michels 1976), CeO_2 (Stringer *et al.* 1972*b*; Wright *et al.* 1975), Sm_2O_3 (Stringer & Hed 1971) and ThO_2 (Davis *et al.* 1971; Giggins & Pettit 1971; Lowell *et al.* 1971; Wallwork & Hed 1971; Lowell 1972; Lowell & Saunders 1972; Wright *et al.* 1975; Michels 1976). Interest in the latter addition stems from the development of ThO_2-dispersion strengthened nickel as a high temperature material and attempts to improve its oxidation resistance by addition of chromium: TDNiC (trade name, Fansteel Inc., for Ni–20Cr–2 %ThO_2 by volume) is now a commercially available material.

With the exception of Li_2O, which had little effect, all of the other dispersed oxides markedly improved the oxidation resistance of Ni–20Cr. Essentially the rate of growth of the Cr_2O_3 scale is reduced, although it is difficult to quantify this. First, for alloys of this type fabricated via a powder metallurgical route there is considerable sample to sample scatter; secondly, surface preparation is also important with polished samples generally oxidizing faster than abraded surfaces, and finally the grain size of the material is also important (Stringer *et al.* 1972*b*; Giggins & Pettit 1971; Wright *et al.* 1975). However, Giggins & Pettit (1971) suggest that although the oxidation kinetics at 900 and 1000 °C do not obey a parabolic rate law in the early stages, this law is approached at longer times and the rate constant for Ni–20Cr–2 %ThO_2 (by volume) is about an order of magnitude less than that of Ni–30Cr. Stringer *et al.* (1972*b*), on the other hand, comment that the rate of growth of the scale appears to be reduced even in the early stages of oxidation. Figure 1 shows typical oxidation data for TDNiC oxidized in oxygen at a partial pressure of 0.1 atm (*ca.* 10^4 Pa) (Giggins & Pettit 1971); data for Ni–30Cr are also included for comparison.

The overall temperature dependence of the oxidation of dispersion-containing alloys is not very great and this is illustrated in figure 2 which shows typical rate curves at 900, 1000, 1100 and 1200 °C for Ni–20Cr–2 %Y_2O_3 (by volume) alloys (Stringer *et al.* 1972*b*). This slight temperature dependence is a combination of two factors: first, the growth rate of Cr_2O_3 is only marginally reduced at lower temperatures by the presence of the dispersoid, and secondly, as the temperature is increased, the oxidation kinetics are complicated further by the oxidation of Cr_2O_3 to the volatile species CrO_3. Thus the rate curves at 1100 and 1200 °C represent the result of two opposing processes: growth of the oxide, determined by transport across the scale and oxidation–volatilization of Cr_2O_3 at the gas–scale interface, which is independent of scale thicknesses. Similar phenomena have been observed during the oxidation of chromium (Lewis

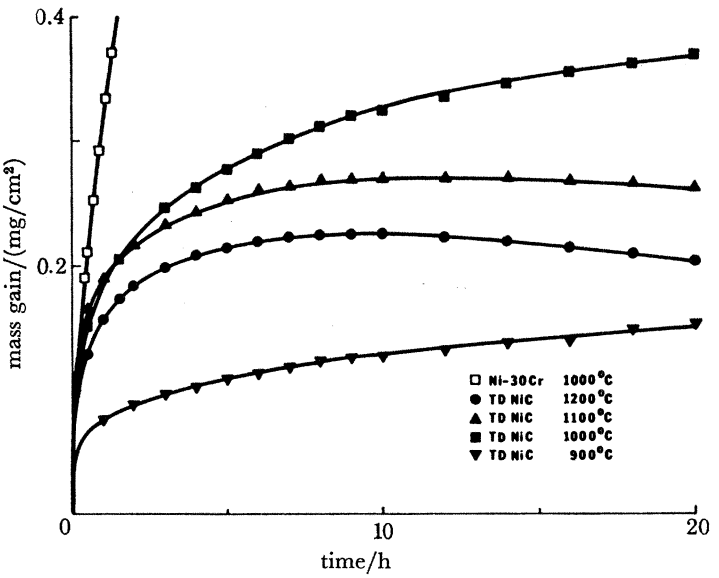

FIGURE 1. Typical mass gain–time data for the oxidation of TDNiC (Ni–20Cr–2 %ThO_2 by volume) in static oxygen at 0.1 atm (*ca.* 10^4 Pa) pressure. (Giggins & Pettit 1971.)

1965; Tedmon 1966): the overall mass change curve rises to a maximum, and then diminishes, samples eventually losing mass at a constant rate. The scale thickness tends asymptotically to a constant value. With alloys containing a dispersoid, the maximum in the rate curves always occurs much earlier than it does with dispersion-free alloys, and the limiting scale thickness is much reduced. Thus the growth rate of the Cr_2O_3 must be lower on the dispersion-containing alloys if the rate of volatilization is unaffected: this seems to be so (Davis *et al.* 1971; Giggins & Pettit 1971; Stringer *et al.* 1972*b*; Wright *et al.* 1975). More detailed analysis of the kinetic curves (Stringer 1972) suggests that a further effect of a dispersed oxide phase is to alter the form of the growth law of the oxide.

Inert Pt markers placed on Ni–20Cr–2 %ThO_2 (by volume) (Giggins & Pettit 1971; Wallwork & Hed 1971) or Ni–20Cr–3 %Y_2O_3 (by volume) (Stringer *et al.* 1972*b*) were found at the scale–gas interface after oxidation; on a dispersion-free alloy, Ni–30Cr, they were found at

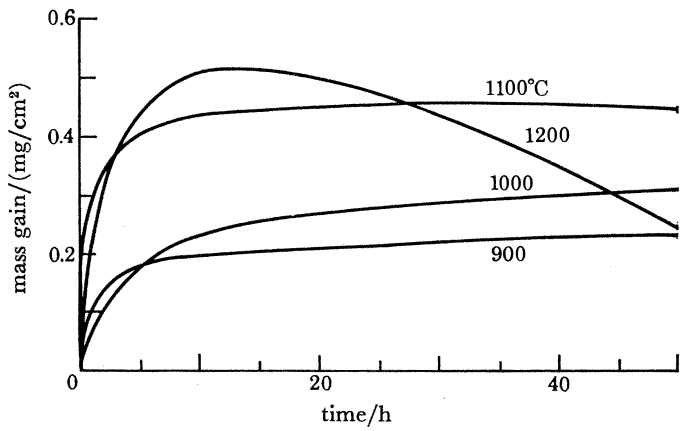

FIGURE 2. Temperature dependence of the oxidation of Ni–20Cr–3 %Y_2O_3 (by volume) alloys in oxygen at 100 Torr (*ca.* 13300 Pa). (Stringer *et al.* 1972*b*.)

the alloy–scale interface and so clearly some change in growth mechanism due to the dispersoid is involved.

In addition, Giggins & Pettit (1971) observed that ThO_2 particles from TDNiC were found throughout the scale, except for scales grown for only short times. Wright & Seltzer (1973), using ion-probe microanalysis, found thorium and yttrium distributed throughout the whole thickness of the scale but were unable to distinguish whether this was present as an oxide dispersion or in solution in the scale. Generally the Cr_2O_3 oxide grain size was some five to ten times smaller over dispersoid-containing material than over dispersion-free material (Stringer *et al.* 1972*b*); the oxide grain size was also quite stable and changed little with continued exposure (Wright *et al.* 1975).

Stringer *et al.* (1972*b*) found that considerably less nickel-rich oxides were formed on Ni–20Cr alloys containing an oxide dispersion, 3 %Y_2O_3 or Ce_2O_3 (by volume), in comparison with the same alloy without the oxide addition, and it appeared as if the presence of the dispersoid increased the rate at which a continuous protective layer of Cr_2O_3 was developed in the early stages of exposure. This was even more marked with Ni–13.5Cr–1ThO_2 which in some cases was able to develop a Cr_2O_3 scale: this would have been impossible at this chromium level in the absence of the dispersoid (Davis *et al.* 1971). However, a 2.5 % Sm_2O_3 dispersion had no effect on Ni–7.5Cr (Stringer & Hed 1971).

Finally, as with active element additions, the dispersed oxides promote good scale adherence. This is evident both from cyclic oxidation tests (Wright *et al.* 1975; Michels 1976) and from the reduction in scale spallation at the end of isothermal exposures.

A number of workers have studied the oxidation behaviour of pure chromium containing either yttrium (Hagel 1963) or a dispersion of Y_2O_3 (Seybolt 1966) or ThO_2 (Stringer *et al.* 1972*a*). Y as a 0.9 % metallic addition had little effect on the parabolic rate of oxidation, but between 900 and 1075 °C there was a significant reduction in the degree of blistering of the scale and an improvement in adhesion at higher temperatures. Seybolt (1966) found that Cr–5 %Y_2O_3 (by volume) oxidized initially according to a parabolic rate law in the temperature range 1150–1370 °C but then there were negative deviations from this after about 200 min. Tentative evidence suggested that the double oxide $YCrO_2$ formed at the scale–alloy interface. The oxidation behaviour of Cr–3.12 %ThO_2 was in agreement with the observations of Ni–20Cr–ThO_2 alloys referred to above: the rate of oxidation at 1100 and 1200 °C was significantly reduced by the dispersoid and the oxide scale had a somewhat smaller grain size. However, the ThO_2 particles tended to accumulate at the metal–oxide interface at least in the early stages, which is in contrast to the earlier observation by Giggins & Pettit (1971).

(*b*) *Alumina-forming alloys*

Early work with Al_2O_3-forming alloys centred around iron-based alloys containing about 25 % Cr and 5 % aluminium, which, although relatively weak at elevated temperatures, possessed good resistance to oxidation. Wukusick & Collins (1964) demonstrated that addition of yttrium to this alloy resulted in improved oxidation resistance under cyclic conditions. Other workers have since confirmed that the beneficial effect of Y (Francis & Whitlow 1965; Tien & Pettit 1972; Golightly *et al.* 1976) or Sc (Tien & Pettit 1972) additions to alloys of similar or lower chromium contents, Fe–15Cr–4Al (Antill & Peakall 1967; Francis & Jutson 1968) is related to the improved scale adherence. In fact, the oxidation rate under isothermal conditions is little affected, and might even be increased slightly in the presence of the addition owing to

these providing rapid diffusion paths in the form of yttria and scandia stringers in the scale (Tien & Pettit 1972).

Tien & Pettit (1972) noted that inert platinum markers placed on the surface of the alloy before oxidation were always found at the gas–oxide interface irrespective of whether the alloy contained additions or not. However, there were morphological differences in the Al_2O_3 scales formed on the two types of alloy. The first feature was the lack of voids at the oxide–substrate interface under the adherent Al_2O_3 scale formed on the Sc- or Y-containing alloy, and the second feature was the relative smoothness of the Al_2O_3 scale at the gas–oxide interface. In addition, stringers of Sc_2O_3 or Y_2O_3 were found to penetrate into the alloy from the scale, although these were completely incorporated into the scale after prolonged exposures. In contrast, the non-adherent Al_2O_3 scales formed on the addition-free alloys had a dimpled outer surface containing numerous filamentary protrusions and ridges. Large cavities were observed between scale and substrate and in places the alloy substrate showed smooth areas, not imprinted with oxide grains as was the remainder of the surface. These smooth areas were not completely featureless but contained steps typical of thermal etching.

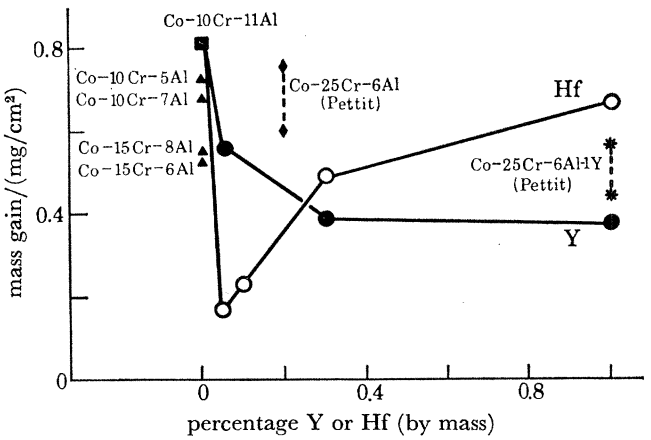

FIGURE 3. The effect of Hf and Y content in Co–10Cr–11Al on the mass gain after 100 h exposure at 1100 °C in air. (Allam *et al.* 1978*a*; Giggins & Pettit 1975.)

Golightly *et al.* (1976) noted that the Al_2O_3 scale on Fe–27Cr–4Al developed what was described as a convoluted morphology and the formation of ridges of oxide within the scale. These ridges apparently grew with increasing exposure time. The scale on Fe–27Cr–4Al–Y alloys, on the other hand, did not show detachment from the alloy, or ridge formation.

Yttrium and hafnium additions to Co–10Cr–11Al alloys appeared to decrease the isothermal oxidation rate at 1100 °C (Stringer *et al.* 1977; Allam *et al.* 1978*a*), although Giggins & Pettit (1975) maintained that Y additions to Co–25Cr–6Al had virtually no affect under isothermal conditions. These latter authors suggested the oxidation rate fitted a parabolic rate law. Allam *et al.* (1978*a*), however, showed that although undoped Co–10Cr–11Al followed an approximate parabolic law, the oxidation rate of the Hf- or Y-doped alloys decreased at a much faster rate than was consistent with diffusion-controlled growth. Furthermore, increasing the Hf and Y content tended to reduce the duration of the initial transient oxidation stage and speed up the establishment of a continuous Al_2O_3 layer. Figure 3 compares the mass gain after 100 h exposure at 1100 °C for the various alloys. On the undoped alloys, the mass gain ranges from

0.53 to 0.82 mg/cm^2: there is no real systematic variation with alloy composition, although the higher chromium content alloys are perhaps slightly better. For additions of Hf the maximum effect is with the smallest hafnium addition. Under thermal cycling conditions, the maximum effect was obtained at higher hafnium levels, 0.3–1.0 %.

Metallographic evidence indicated differences between the doped and undoped alloys (Giggins & Pettit 1975; Stringer *et al.* 1977; Allam *et al.* 1978*a*) similar to those referred to above for Al_2O_3-forming iron-based alloys. First, the alloy surface after the Al_2O_3 scale had been removed was completely covered with imprints of the oxide grains for the doped alloys whereas there were numerous smooth areas, representing areas of no contact between scale and alloy, for the ternary alloys. Examples of these are shown in figure 4, plate 1. A 0.05 % addition was sufficient to eliminate these voids.

The second major difference was the presence of intrusions of oxide growing into the alloy from the surface scale. These intrusions were principally Al_2O_3 that had grown around particles of internally formed active element oxide. The morphology of the oxide intrusions was different for Y- and Hf-containing alloys, and alloys containing an HfO_2 dispersion and these are compared in figure 5, plate 2. These latter had been prepared by internal oxidation of Co–10Cr–11Al–Hf in a low oxygen activity pack such that only Hf, and not Cr or Al, were converted to oxide (Allam *et al.* 1978*b*). In Y-containing alloys the protrusions are relatively large and infrequent along the alloy–scale interface and their distribution is related to that of the intermetallic yttride in the alloy. With the Hf-containing alloys the Al_2O_3 intrusions were more profuse and consisted of branching growths penetrating into the alloy. A number of large penetrations developed with the Hf-containing alloy, but not with the alloy containing an HfO_2 dispersion. Also with this latter alloy, the distribution of the internal stringers was on a finer scale. The concentration of oxide intrusions increased with active element content of the alloy.

Kuenzly & Douglass (1974) studied the effect of 0.5 % Y on the oxidation behaviour of Ni_3Al (Ni–13.2 %Al): the mass gains for the Y-containing alloy were consistently 10–20 % higher than corresponding undoped alloys. Yttrium additions to Ni–8Cr–6Al (Kvernes 1973) or Ni–10Cr–5Al (Kumar *et al.* 1974), however, reduced the isothermal oxidation rate. A 0.5 or 1.0 % Th addition had the opposite effect (Kumar *et al.* 1974). In all cases, the additions of Y or Th provided increased resistance in thermal cycling tests, as did additions of 2.5–10 %Pt or 5 % Rh, but not 5 % Au (Felten 1976). It was suggested (Kumar *et al.* 1974) that in the presence of yttrium, mixed oxides $YAlO_3$ and the garnet $Y_3AL_5O_{12}$ were formed in addition to Al_2O_3.

As noted earlier for cobalt-based alloys, the presence of the active metal addition suppressed the development of smooth areas on the substrate surface, implying that cavity formation between scale and alloy has been eliminated (Giggins *et al.* 1974; Kumar *et al.* 1974; Kuenzly & Douglass 1974; Giggins & Pettit 1976). In addition, Giggins *et al.* (1974) noted that an Al_2O_3 scale developed much more readily on a Ni–15.1 %Ta–6.7 %Al alloy doped with 0.04 % Y than on a similar undoped alloy. In spite of this improvement in the perfection of the oxide–substrate interface, the scale spalled from this alloy during cooling. Doping of the same alloy with 1.5 % Hf instead of yttrium prevented scale spallation, and examination in cross section revealed a profusion of oxide platelets extending from a relatively uniform scale into the substrate.

Seltzer *et al.* (1972) developed a pack diffusion process permitting the introduction of approximately 6 % Al into solid solution in the near surface region of TDNiC or Ni–20 %Cr.

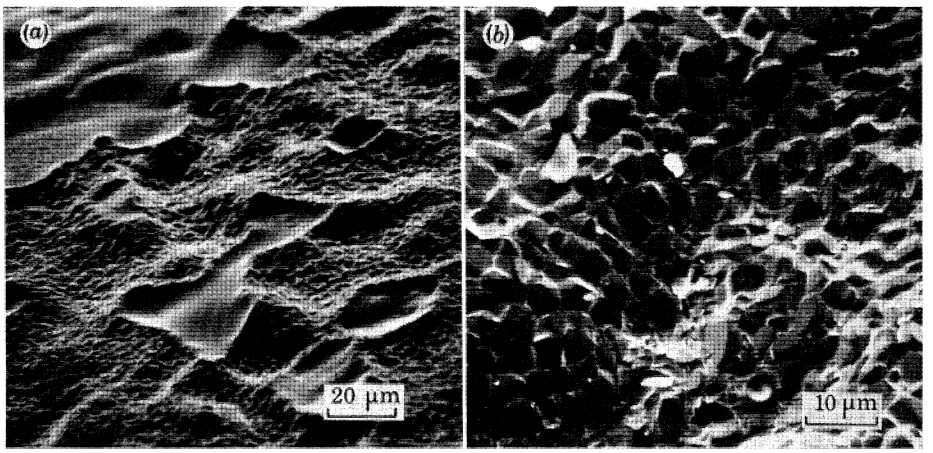

FIGURE 4. The alloy surface after removal of the scale of a specimen of (*a*) Co–15Cr–8Al oxidized for 190 h at 1200 °C and (*b*) Co–10Cr–11Al–0.1Y oxidized for 1000 h at 1200 °C. The surface of the Y-containing alloy is completely imprinted with oxide grains; that of the Y-free alloy contains smooth, imprint-free regions where the scale was not in contact with the alloy. (Allam *et al.* 1978*a*.)

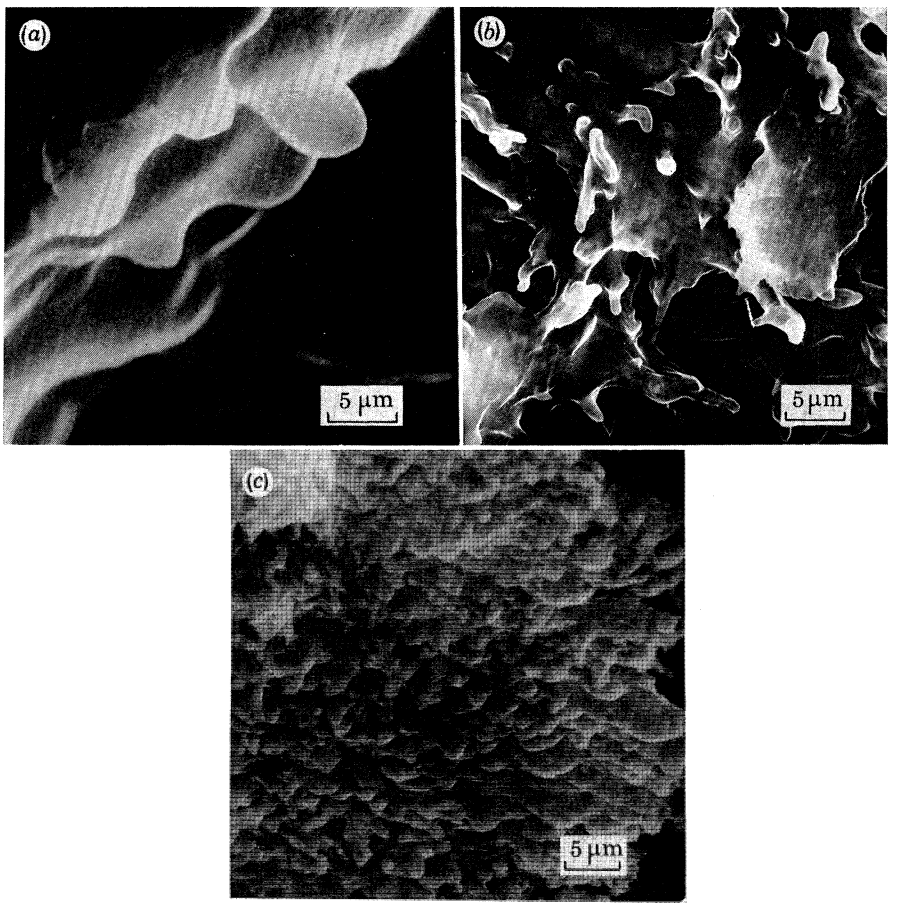

FIGURE 8. A comparison of the underside of the Al_2O_3 scale, stripped from the alloy. (*a*) Co–10Cr–11Al–0.3Y oxidized for 75 h at 1200 °C. (*b*) Co–10Cr–11Al–1Hf oxidized for 75 h at 1200 °C. (*c*) Co–10Cr–11Al–1Hf, internally oxidized in a CoAl–Al_2O_3 mixture for 200 h at 1200° C to convert the Hf into an oxide dispersion, and then oxidized for 75 h at 1200 °C. (Allam *et al.* 1978*b*.)

(*Facing p.* 316)

PHILOSOPHICAL TRANSACTIONS OF THE ROYAL SOCIETY A MATHEMATICAL, PHYSICAL & ENGINEERING SCIENCES

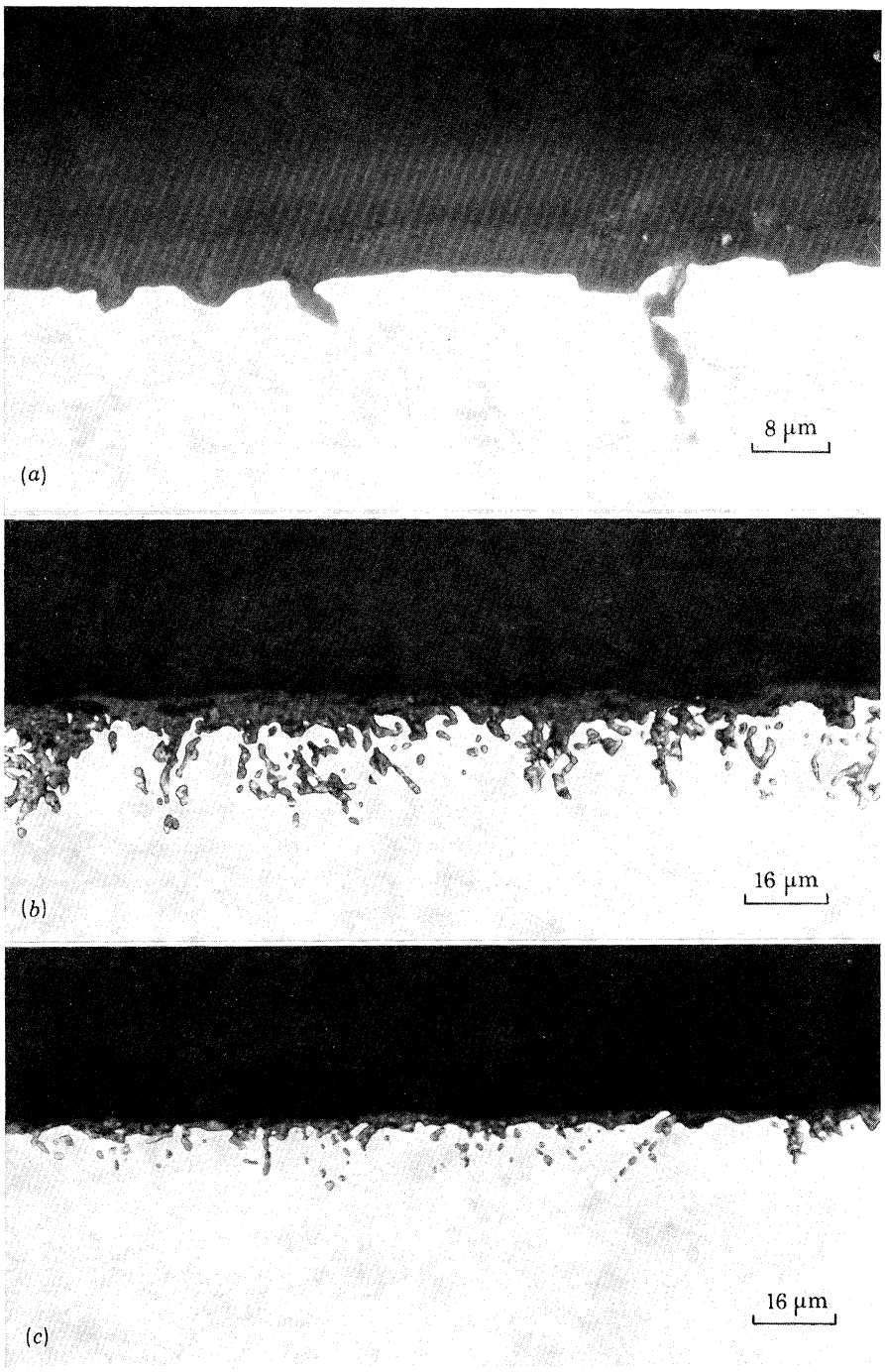

FIGURE 5. A comparison of the morphology of oxide peg development: (*a*) Co–10Cr–11Al–1Y oxidized for 1000 h at 1200 °C; (*b*) Co–10Cr–11Al–1Hf oxidized for 350 h at 1200 °C; (*c*) Co–10Cr–11Al–1Hf internally oxidized in a $CoAl–Al_2O_3$ mixture for 200 h at 1200 °C to convert the Hf into an oxide dispersion, and then oxidized for 350 h at 1200 °C.

The intrusions in the Y-containing alloy are relatively large and infrequent along the interface. In comparison, the Hf-containing alloy contains profuse intrusions which can grow quite large, while the HfO_2-containing alloy has a finer, more regular distribution. (Allam *et al.* 1978*b*.)

The ThO_2-containing alloy exhibited superior oxide scale adhesion during cyclic testing: similar oxidation kinetics for the two alloys were observed under isothermal conditions.

3. Beneficial effects of additions

The 'rare earth effect', then, is made up of a number of different factors, some of which are clearly interrelated:

1. Selective oxidation of the protective scale-forming element, aluminium or chromium, is enhanced, particularly during the early stages of exposure, with the result that (*a*) a continuous layer of Cr_2O_3 or Al_2O_3 is formed at a lower chromium or aluminium content on alloys containing additions than addition-free alloys: this is more marked for Cr_2O_3-forming alloys and especially systems (e.g. Co–Cr) in which relatively high levels of chromium are normally required; and (*b*) the transient oxidation stage is curtailed and less base metal oxidation occurs.
2. The growth rate of Cr_2O_3 scales is undoubtedly reduced at high temperatures (not less than 1000 °C) and that of Al_2O_3 scales may be reduced.
3. The transport mechanism of Cr_2O_3 is altered in the presence of an oxide dispersion in the alloy from predominantly metal transport to predominantly oxygen transport; there is no real evidence to suggest a similar change with Al_2O_3, for which oxygen transport, apparently via grain boundary short circuit paths, appears to be the dominant transport mechanism in the absence of a dispersion.
4. Void formation at the alloy–Al_2O_3 interface is suppressed virtually completely for alloys containing additions; there may be a similar reduction with Cr_2O_3-forming alloys, but it is not complete.
5. The adherence of the scale to the alloy is increased in both cases.

A wide variety of metallic or oxide dispersoid additions produce all or most of these effects to differing degrees. The main critical factor appears to be that a potential metallic addition must have a higher affinity for oxygen than the element that is to form the protective scale; an oxide addition must be at least as stable, and preferably more stable, than the scale. Thus an Al_2O_3 dispersion is suitable for Cr_2O_3-forming alloys, but the reverse would not be true (although this system has not been investigated).

It has not been clearly established whether the effect of adding a reactive element to an alloy is identical to that of adding a stable oxide dispersion. Certainly the effects of the latter are usually more dramatic. In alloys containing reactive element additions only, it is probable that the reactive element oxidizes internally ahead of the scale–alloy interface, but this is unlikely to have any effect in the early stages of oxidation.

4. Initial development of the protective scale

In attempting to explain the influence of dispersed oxide additions in the early, transient stages of oxidation, Stringer *et al.* (1972*b*) suggested that the dispersed particles in the alloy surface acted as nucleation sites for the first formed oxides, thus decreasing the internuclei spacing. The model is summarized in figure 6, by using a Ni–20Cr alloy with and without a 2% ThO_2 (by volume) addition as an example. The dispersoid represents a surface discontinuity, and it is not necessary to postulate that the dispersoid preferentially acts as nucleation sites for Cr_2O_3 (or Al_2O_3). By decreasing the distance between adjacent Cr_2O_3 (or Al_2O_3)

nuclei, the time required for the lateral growth process to form a complete layer of that oxide and terminate the formation of base-metal oxides, is reduced. Direct experimental evidence for this model is difficult to obtain: the grain size of the oxide over the dispersion-containing material has been found to be between five to ten times smaller than over dispersion-free material, in accord with the model (Stringer *et al.* 1972*b*; Wright *et al.* 1975). Furthermore, Flower & Wilcox (1977), using in-situ oxidation of TDNiC in a high-voltage microscope, showed some evidence that ThO_2 particles acted as preferential nucleation sites for oxidation. However, metal grain boundaries, slip steps and other inclusions were equally effective.

It seems also that Y_2O_3 additions to alumina can stabilize a fine-grained structure. Nanni *et al.* (1976) found that Y_2O_3 segregates to the grain boundaries at monatomic layer levels, and permits full theoretical density to be achieved by stabilizing the fine-grained structure.

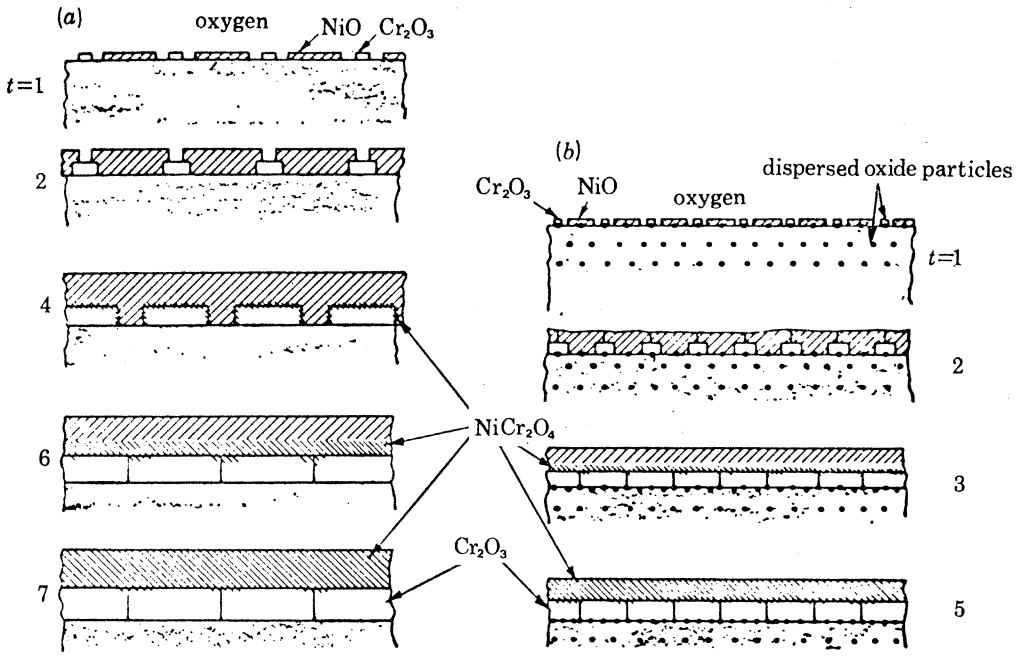

FIGURE 6. Schematic diagram illustrating how dispersoid oxide particles, by acting as nucleation sites for the first-formed oxide, accelerate the approach to steady state and reduce the amount of nickel-containing oxides in the oxidation of Ni–20%Cr (*a*) without and (*b*) with 2–3% (by volume) dispersed oxide particles. (Stringer *et al.* 1972*b*.)

Metallic additions have less effect in the early stages: Antill *et al.* (1976) in long-term exposure tests on 20/25 CrNiNb steels, ion-implanted with Y, at 800–850 °C in CO_2 showed that the extents of nucleation and film growth during the initial 300 h were comparable on Y-free and Y-bearing steels. In Fe–25Cr, however, there was a marked change in the initial oxidation rate by the addition of 1% Y, but 5% Al produced a similar change (Francis & Whitlow 1965). Wright *et al.* (1975) indicated that selective oxidation of chromium from Ni–20Cr occurred on alloys containing Y additions, dispersion-free alloys as well as alloys containing an oxide dispersion, and they suggested that the chromium diffusion rate in the alloy was enhanced by the fine grain size which encouraged the rapid growth of the original Cr_2O_3 nuclei into a continuous layer. Both active metal and oxide dispersions tend to stabilize a fine alloy grain size; furthermore, the Ni–20Cr alloy used in their work was made by a powder metallurgical

route and had a similar fine grain size. The fine sub-grain boundaries are rapid diffusion paths for chromium (Fleetwood 1966), and chromium diffusion in these alloys can vary by an order of magnitude depending on the grain size (Seltzer 1972; Seltzer & Wilcox 1972). However, Seltzer (1972) pointed out that the presence of the dispersoid has no other effect on the diffusion in the alloy.

Undoubtedly the alloy interdiffusion rate is important in these early stages of oxidation when the protective scale is developing, as also are surface finish and the rate of heating the sample to the oxidizing temperature (Wood 1971). Giggins & Pettit (1969) have shown, for example, that Cr_2O_3 develops on Ni–Cr alloys more readily over alloy grain boundaries than over the bulk of the grains, and on cold-worked surfaces than on polished ones. Equally, more nickel-rich oxides formed on metallographically polished samples of TDNiC than on samples which had been mechanically ground (Lowell 1972). However, other surface conditions being equal, the nucleation effect is probably overriding as indicated by one further piece of evidence. As described above, alloys containing an oxide dispersion are able to develop a continuous Cr_2O_3 scale at lower alloy chromium contents than similar alloys in the absence of a dispersoid. Whittle *et al.* (1977) oxidized Co–15Cr alloys containing 1 % Ti, Zr or Hf in the temperature range 1000–1200 °C and a continuous Cr_2O_3 scale was not formed. If, however, the reactive element addition was first converted to an oxide dispersion, and this was achieved by a controlled internal oxidation treatment in a sealed pack in which the oxygen activity was sufficiently low to oxidize the reactive element only, then on subsequent exposure a continuous protective Cr_2O_3 layer was formed. This presumably is a direct consequence of the smaller internuclear spacing in the initial stages of oxidation. There was no change in alloy grain size as a result of the internal oxidation and it is clear that this cannot be a major effect; equally, it is unlikely that much substructure was generated by this treatment. Thus, in terms of the initial development of the protective oxide scale, oxide dispersions are clearly more beneficial than corresponding active metal additions. It should be appreciated however, that in the latter alloys, a significant proportion of the active metal addition may well be present as oxide, formed during the melting and casting operations.

The lower limit to which the chromium content of this type of alloy can be reduced seems to be about 13 %, and is the same in Fe, Ni or Co-based alloys (Davis *et al.* 1972; Stringer & Hed 1971; Whittle *et al.* 1977). Interestingly, stable nitride dispersions have a similar effect, at least in Fe–Cr alloys (Goncel *et al.* 1978).

There is less effect either of active element additions or of dispersed oxide phases in Al_2O_3-forming alloys during the initial stages of oxidation. This is probably related to the fact that most Al_2O_3-forming alloys also contain substantial amounts of chromium which also seem to aid the establishment of the Al_2O_3 layer. Equally, it is doubtful whether there is much scope for further reduction in the alloy aluminium content necessary for a continuous Al_2O_3 scale, since with most systems this is already close to 5 %. Kvernes (1973) did suggest that selective oxidation of aluminium from a Ni–9Cr–6Al alloy during the early stages of exposure was promoted by additions of up to 0.7 % Y because of the higher diffusion rate in the alloy as a result of the stable substructure. However, the evidence is not particularly convincing. Allam *et al.* (1978*a*) also found less development of Co-rich oxides before the establishment of an Al_2O_3 scale on Co–10Cr–11Al containing up to 1 % Y or Hf. The kinetic curves showed a rapid initial mass gain, but this flattened off very quickly. In comparison, the same alloy without an addition showed a lower mass gain initially, but there was no abrupt decrease in the rate. The same

PHILOSOPHICAL TRANSACTIONS OF THE ROYAL SOCIETY A MATHEMATICAL, PHYSICAL & ENGINEERING SCIENCES

alloys given a pre-internal oxidation treatment in a low oxygen activity pack, to convert the active element to a dispersion, showed similar, but even more pronounced, changes in the oxidation kinetics in the early stages (Allam *et al.* 1978*b*).

5. Scale growth

Essentially three main mechanisms have been proposed to explain the reduction in scale growth rate and possible modification to the transport process brought about by metallic or oxide additions. They refer mainly to Cr_2O_3 scales since, as indicated in §2, it is not entirely clear whether there is any real reduction in rate with Al_2O_3. The mechanisms are: (*a*) doping effects; (*b*) formation of a partial or complete blocking layer in the scale; and (*c*) short-circuit diffusion models.

Francis & Whitlow (1965) suggested that a 1% Y addition to Fe–25Cr may modify the Cr_2O_3 structure so that the cation diffusion rate through the scale is reduced. However, yttrium is trivalent and no doping effect would be expected if this element dissolved in Cr_2O_3. Substitution of thorium or cerium which can have valencies of four may affect the transport rate: there is some evidence that at temperatures above about 1200 °C, Cr_2O_3 is an intrinsic electronic conductor (Kofstad 1972), in which case substitution of thorium or cerium in the Cr_2O_3 lattice would lead to a reduction in the concentration of interstitial chromium ions and so to a reduction of the outward transport of chromium, eventually leading to n-type behaviour. Michels (1976), however, comments that Cr_2O_3 is a p-type semiconductor (Hauffe & Block 1951; Lorenz & Fischer 1958; Hagel & Seybolt 1961) also containing Frenkel pairs (Hagel & Seybolt 1961). Thus, dispersoids such as Y_2O_3, La_2O_3, ThO_2 and Al_2O_3, in which the metal is capable of assuming a trivalent state and occupying cation vacancies, improve the oxidation resistance: the total defect content of Cr_2O_3 is reduced. Introduction of atoms capable of assuming a monovalent state, such as lithium in Li_2O, would be expected to have little or no effect. The main weakness of the doping argument lies in the apparently equal efficacy of a wide range of both metallic and oxide dispersion additions.

Wood & Boustead (1968) suggested that the asymptotic growth rate obtained by additions of Y or Gd to Fe–Cr alloys were more readily explained by some time-dependent phenomenon, for example, the development of a layer of compound such as $YCrO_3$ or Y_2O_3 at the oxide–alloy interface. Detailed investigation was unable to detect a complete layer, although a Y-rich compound was found along about 50% of the scale–alloy interface. Beltran (1970) indicated the reduced oxidation rate of Co–30Cr containing 1% Y might be explained in terms of a reduction of chromium flux towards the interface owing to the precipitation of rare earth oxides in the alloy matrix acting as a 'set of sieves in series' blocking the supply of chromium. Kumar *et al.* (1974) detected the formation of the double oxides $YAlO_3$ and $Y_3Al_5O_{12}$ during the oxidation of Ni–12Cr–3Al, a Cr_2O_3-forming alloy. The double oxides were present as discrete particles (mostly at grain boundaries) and not as a continuous layer. However, it was thought that these particles may provide a small, but additional barrier to the diffusing species and thereby reduce the oxidation rate. Such oxides were also detected on an Al_2O_3-forming alloy, Ni–10Cr–5Al, but the oxidation rate of this alloy was unaltered: presumably the protectiveness offered by the mixed oxides is comparable with that offered by Al_2O_3.

Giggins & Pettit (1971) proposed a model in which the incorporation of the dispersoid particles in the scale supposedly reduces its growth rate by decreasing the cross sectional area

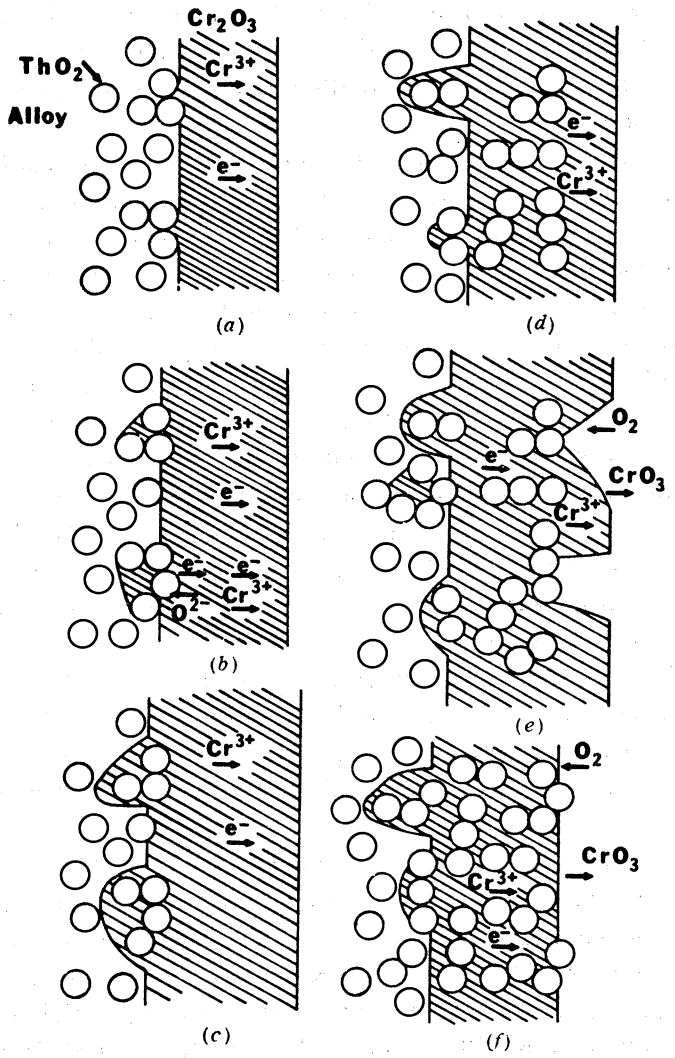

FIGURE 7. Schematic diagram of the model for the oxidation of TDNiC. (*a*) A thin layer of Cr_2O_3 is formed via the outward diffusion of chromium, and the alloy–Cr_2O_3 interface becomes filled with agglomerates of ThO_2 particles. (*b*) The ThO_2 agglomerates prevent the movement of chromium from the alloy and the Cr_2O_3 dissociates. Cr_2O_3 is formed beneath the ThO_2 agglomerates by the diffusion of oxygen through these particles. (*c*) The Cr_2O_3 formed beneath the thoria by the dissociation reaction becomes joined to the external scale upon continued growth of this type of Cr_2O_3 as well as growth of the external scale. (*d*) The inward growth mode that is caused by the agglomerated ThO_2 particles and the outward growth mode resulting from the diffusion of chromium in Cr_2O_3 produce a two-zoned Cr_2O_3 scale. (*e*) Portions of the outer zone are removed by the formation of CrO_3. (*f*) After long periods of oxidation virtually all of the outer zone is removed by the vaporization reaction. The ThO_2 particles in the Cr_2O_3 decrease the oxidation rate by decreasing the cross sectional area of Cr_2O_3 available for the transport of chromium. (Giggins & Pettit 1971.)

of Cr_2O_3 available for transport of chromium. Initially, in the oxidation of TDNiC, a thin layer of Cr_2O_3 is formed via the outward diffusion of chromium, and the alloy–Cr_2O_3 interface becomes filled with agglomerates of ThO_2 particles. This is shown schematically in figure 7. The ThO_2 agglomerates prevent the movement of chromium from the alloy and the Cr_2O_3 dissociates. Cr_2O_3 is formed beneath the agglomerates by the diffusion of oxygen through these particles. Continuation of this process results in a two-zone Cr_2O_3 scale. Eventually, the outer

zone of oxide is removed by volatilization. Thus, this model also explains why the platinum markers are found at the scale–gas interface: the scale is formed by both and inward and outward growth processes and the vaporization eventually removes most of the Cr_2O_3 layer formed via the outward growth mode.

Elegant as this model may be, it probably falls down because even relatively small additions can produce significant reductions in the oxidation rate and this would require a very considerable reduction in cross sectional area. This, then, led Stringer *et al.* (1972*b*) to suggest that the dispersoid may only block short-circuit diffusion paths for chromium. These are not grain boundaries, which in ionic solids are short-circuit paths for anions and not cations (Laurent & Benard 1958), but dislocations, as possibly also occur in Fe_2O_3 (Tallman & Gulbransen 1968). The presence of the dispersoid in the alloy reduces the oxide grain size: if it is reduced below a level corresponding to the interdislocation distance in a pile-up, a single dislocation is not stable within the grain and will move to the grain boundary, where it ceases to be a cation diffusion path. Thus, if the short-circuit diffusion paths for chromium in Cr_2O_3 are dislocations, reducing the grain size of the oxide below certain limits may reduce the density of the paths and hence the diffusion rate. Equally, the oxygen diffusion rate via grain boundaries will be increased and a reversal in growth process will occur, with the oxide forming reaction shifting from the oxide–gas interface to the oxide–metal interface, as is indeed observed.

Two-stage oxidations of austenitic steels with the use of ^{16}O and then ^{18}O (Lees & Calvert 1976) indicate that there is some change in scale growth mechanism when a TiN dispersion is present in the alloy. The contribution of inward oxygen transport is increased but the evidence suggests that the new oxide may well be formed within the scale, rather than at either of the interfaces.

Golightly *et al.* (1976) suggest a similar type of mechanism for Al_2O_3 growth. In addition-free alloys, both cation and anion transport contribute to Al_2O_3 growth with the formation of new oxide within the existing oxide layer. Additions of Y to the alloy are incorporated into the oxide and suppress cation transport. This has only a minor effect on the growth rate in this instance since in Al_2O_3 it is the slower process that is suppressed. However, it might explain the improvements in scale–alloy adhesion as will be discussed in §6. Nanni *et al.* (1976) suggest that the segregation of yttria to the grain boundaries during the sintering of Y_2O_3-doped Al_2O_3 may reduce the grain boundary transport rates, presumably of oxygen ions: certainly, sintering rates are reduced.

Unfortunately, sufficiently precise data are not available to compare the actual transport rates during oxidation with those expected for bulk or short-circuit diffusion.

6. Scale–alloy adherence

Improvement in scale–alloy adherence has been the aspect studied in most detail, and a number of hypotheses have been put forward to account for this. Essentially, these are independent of whether the alloy contains a metallic addition of the active element or a dispersion of its stable oxide. As pointed out earlier, because of the high affinity for oxygen of the active elements, they will be oxidized preferentially to chromium or aluminium, and as the addition is only present at a low concentration, the resulting oxides are in the form of discontinuous internal oxide particles in the alloy substrate ahead of the oxide–alloy interface. The distribution of the oxides may be very different in the two cases: those formed during high temperature oxidation are

often formed in the vicinity of alloy grain boundaries at intersections with the scale–alloy interface. In dispersion-containing alloys, the distribution is generally more random.

The most important mechanistic models explaining the improved scale adherence, although it must be realized that these are not necessarily mutually exclusive, are: (*a*) enhanced scale plasticity; (*b*) graded seal mechanism; (*c*) modification to growth process; (*d*) chemical bonding; (*e*) vacancy sink model; (*f*) oxide pegging.

(*a*) *Enhanced scale plasticity*

It has been proposed (Antill & Peakall 1967; Francis & Jutson 1968; Pettit 1972) that elements such as yttrium may improve the adhesion of Al_2O_3 on alloys by causing the Al_2O_3 to be more easily deformed and thereby allowing the relief of growth and thermally induced stresses that would otherwise have caused spallation of the Al_2O_3. Grain boundary sliding is expected to be the major deformation mechanism in the scale, and it has been suggested that a fine-grained oxide can more easily accommodate growth and thermally induced stresses by grain boundary sliding than larger grained oxide (Tien & Pettit 1972). Kuenzly & Douglass (1974), however, have suggested that the oxide scale plasticity is actually decreased by the addition of yttrium since Y_2O_3, $YAlO_3$ and $Y_3Al_5O_{12}$ (YAG-garnet) form at grain boundaries and inhibit plastic deformation of α-Al_2O_3 by a grain boundary sliding mechanism.

Hollenberg & Gordon (1973) studied the effects of different dopants on the creep behaviour of polycrystalline Al_2O_3 and found that doping with either Fe^{2+} or Ti^{4+} resulted in the creation of either Al-ion interstitials or Al–ion vacancies respectively. Both species enhanced the cation diffusion rate and increased the creep rate. The creep rate of Cr^{3+}-doped Al_2O_3 was comparable to that of undoped Al_2O_3 of similar grain size. Thus, there is no conclusive evidence that the deformability of Al_2O_3 is modified by the incorporation of either active elements, or oxide particles within the scale and it is unlikely that an oxide plasticity model is of particular significance: often there is more apparent deformation of the Al_2O_3 scale on undoped or dispersion-free alloys in any case.

Deformation of the alloy is possibly another means whereby stress relief can occur. Golightly *et al.* (1976) observed apparent deformation of the alloy when a ridged alloy surface developed during Al_2O_3 growth. However, the loads required to deform typical Al_2O_3-forming alloys were not particularly affected by yttrium concentration (Giggins & Pettit 1975).

(*b*) *Graded seal mechanism*

The graded seal mechanism is based on the supposition that a layer of compound oxide is developed between the surface scale and the alloy, which has a thermal expansion coefficient intermediate between that of the scale and the substrate (Pfeiffer 1957). However, as indicated in § 2, there are very few systems in which a complete or even partial layer of a compound oxide has been observed.

(*c*) *Modification to growth process*

As seen in § 5, additions to chromia-forming alloys generally reduce the growth rate of the oxide by a factor of ten or so at elevated temperatures: with alumina-forming alloys there may be a slight reduction in rate, but it is not particularly significant. Any reduction in growth rate might be expected to reduce growth stresses; however, probably of more significance is the actual growth mechanism and it seems fairly clear that the additions to Cr_2O_3-forming alloys

PHILOSOPHICAL TRANSACTIONS OF THE ROYAL SOCIETY A MATHEMATICAL, PHYSICAL & ENGINEERING SCIENCES

promote a contribution from oxygen transport to scale growth and may even make this predominant. Al_2O_3 also grows primarily by oxygen transport, albeit via short circuit paths (Kuenzly & Douglass 1974; Tien & Pettit 1972). Generally, higher levels of growth stress would be expected to be associated with anion-conducting scales (Stringer 1970) since the new oxide is formed under constraint at the alloy–scale interface.

Golightly *et al.* (1976) have suggested that in addition to inward oxygen diffusion down the Al_2O_3 grain boundaries, outward diffusion of aluminium occurs, probably along line defects in the oxide. Reaction between the inward- and outward-diffusing species results in the formation of oxide within the existing scale layer. Hence, lateral growth of the oxide occurs as oxidation proceeds, leading to the rapid development of high compressive stresses and consequent localized detachment of the scale from the underlying alloy. They suggest that condensation of voids (see §6*e*) along the alloy–scale interface and the continuing lateral growth of the scale results in the development of a 'convoluted morphology' of the oxide leading to oxide detachment at temperature and extensive spallation during cooling. Based on this model, the increased adherence of the scale due to Y-additions was mainly attributed to the prevention of the formation of convoluted morphologies: incorporation of yttrium into the scale suppresses the cation contribution to scale growth (see §5) and therefore reduces oxide formation within the existing oxide layer.

D. G. Lees (1978, personal communication) has suggested that the buckling of the Cr_2O_3 scale on pure chromium is also due to the formation of new oxide within the existing layer, and that one effect of an active element addition is to modify this. However, it is also pointed out that when the scale has a columnar structure, the effect may well be less marked.

An alternative proposal explaining the wrinkled morphologies of Al_2O_3 scales (Giggins *et al.* 1974) is related to the growth and impingement of large oxide crystals at the underside of the scale at points where it is detached from the alloy. Aluminium necessary for growth can be easily transported from the alloy across the void via the vapour phase.

The three mechanisms outlined so far are all based on the concept that the effect of the addition produces less stress in the scale–alloy system, or that the system is able to accommodate that stress more effectively. However, Giggins & Pettit (1975) performed the following simple experiment: oxidized samples of CoCrAlY and CoCrAl were bent at room temperature. Scale spallation was far more pronounced from the CoCrAl samples and thus a major effect of the addition is to improve adhesion and any model which proposes improved adhesion because of stress relief or the absence of stress development cannot be wholly acceptable.

(*d*) *Chemical bonding*

The adhesion of the scale to the substrate is clearly dependent upon the nature of the atomic bonds which are developed across the oxide–alloy interface. McDonald & Eberhart (1965) found that impurities that are highly oxygen-active can make a major contribution to the adhesive force at the interface. However, arguing against this being a major factor is the fact that Al_2O_3 dispersions in Cr_2O_3-forming alloys do produce identical improvements in scale adherence: Al_2O_3–Cr_2O_3 solid solutions show little deviation from thermodynamically ideal behaviour. An even more convincing argument is that the presence of an Al_2O_3 dispersion in Fe–25Cr–41Al, an Al_2O_3-forming alloy, also results in a significant increase in adhesion, which obviously cannot be explained in terms of a chemical bonding mechanism (Tien & Pettit 1972).

PHILOSOPHICAL TRANSACTIONS OF THE ROYAL SOCIETY A MATHEMATICAL, PHYSICAL & ENGINEERING SCIENCES

(e) *Vacancy sink model*

There has been clear evidence that the presence of an active metal (Tien & Pettit 1972; Allam *et al.* 1978*a*) or an oxide dispersion in the alloy minimizes the development of voids at the alloy–scale interface; the evidence is not as clear for Cr_2O_3-forming alloys (Francis & Whitlow 1965; Stringer *et al.* 1972*b*; Wright *et al.* 1975). In undoped alloys the voids arise from the condensation of vacancies at the interface and it is proposed (Stringer 1966; Tien & Pettit 1972) that the internal oxide particles of the active element, the active element atoms themselves or the stable oxide dispersion provide alternative sites for vacancy condensation, thus eliminating interfacial porosity. This, in turn, helps to maintain scale–metal contact and minimize scale spallation. The question does arise, however, as to the source of the vacancies. Before it was suspected that the growth direction of Cr_2O_3 scales in the presence of additions might have changed, then the outward diffusion current of metal ions from the metal to the oxide and across the scale produces a countercurrent of vacancies. However, if as indicated in §5, the growth direction is changed, the vacancy source must be elsewhere: Al_2O_3 grows primarily by oxygen transport anyway. Kuenzly & Douglass (1974) have suggested that it might arise from a Kirkendall effect in the alloy substrate, associated with the selective removal of one of the alloy components, and the unequal flux of the more noble components away from the alloy–scale interface. In view of the very slow rates of scale growth, however, particularly with Al_2O_3, such a vacancy flux would be quite small.

There is a further possible source of vacancies: vacancy formation and subsequent development of interfacial voids may be confined to the early, transient stages of oxidation when the faster-growing base metal oxides, NiO, CoO, etc., are being formed. Thus, since active element or stable oxide additions reduce this transient period (§4), there are fewer vacancies to eliminate. Nevertheless, once formed on the addition-free alloys, the voids persist. Allam *et al.* (1978*a*) noted that a 0.05% addition of Y or Hf to Co–10Cr–11Al was sufficient to eliminate the voids completely. However, with such low concentrations of additions the voids did reappear after very long exposures, 1000 h at 1200 °C, but not when the concentration of addition was higher, and this perhaps implies that there is a continuing supply of vacancies and that the vacancy sinks can eventually become saturated.

(f) *Oxide pegging*

Mechanical keying of the oxide to the alloy substrate, as a result of the internal oxidation of the active alloying addition, or dispersoid particles growing in size to form 'oxide stringers' of thin elongated oxide intrusions extending into the alloy substrate, has been suggested by many authors (Lustman 1950; Felten 1961; Wukusick & Collins 1964; Francis & Whitlow 1965; Seybolt 1966; Antill & Peakall 1967; Tien & Pettit 1972; Price *et al.* 1973; Kvernes 1973; Giggins *et al.* 1974; Allam *et al.* 1978*a*, *b*). Earlier models suggested that the oxide peg consisted of the active element oxide itself, or a compound oxide between it and the main scale-forming constituent. However, more recently (Allam *et al.* 1978*a*) it has been shown that the pegs consist primarily of Al_2O_3, at least on Al_2O_3-forming alloys, and form by enhanced inward growth of that oxide along the incoherent boundary between the active element oxide and the metallic substrate.

Giggins & Pettit (1975) differentiate between coarse networks of yttrium-rich oxide protrusions and smaller particles of yttrium-rich oxides: so-called macropegs and micropegs. The

coarse macropegs tend to develop at sites where yttrium-rich intermetallics are present in the alloy. Both micropegs and macropegs serve to key the scale to the alloy mechanically. However, macropegs may not be necessary: prolonged exposure of Fe–24Cr–4.8Al–0.25Sc resulted in all the macropegs being incorporated into the surface scale, yet good scale adhesion was maintained (Tien & Pettit 1972). In fact in alloys containing very low concentrations of yttrium, Fe–24Cr–4.5Al–0.01Y (Tien & Pettit 1972), macropeg formation was not observed, there were no intermetallics in the alloy, but scale adhesion was still good, and better than the equivalent addition-free alloys. It is also suggested (Giggins & Pettit 1972) that alloys containing dispersed oxides do not develop macropegs, presumably for the same reason.

Work by Allam *et al.* (1978*a*, *b*) tends to confirm this. An addition of 0.05% Hf or Y to Co–10Cr–11Al is sufficient to minimize scale spallation and improve overall oxidation resistance under isothermal conditions, but not under thermal cycling conditions. The number of pegs or stringers is important and there are not sufficient in the alloys containing 0.05 and 0.1% Hf; additions of 0.3 and 1.0% Hf appear to be optimum. Higher additions can be detrimental as extra-large pegs can actually promote spallation.

Hafnium additions seem more efficient than yttrium, and this is related to the shape of the pegs as much as to concentration (Allam *et al.* 1978*b*). With the hafnium additions, the internal growth of Al_2O_3 around the Hf-rich internal oxide particles takes on a branched, dendritic form as opposed to the relatively smooth interface between the Al_2O_3 surrounding the Y-rich particles and the alloy. These differences may well be related to the distribution of the active element in the original alloy. Yttrium tends to segregate to grain boundaries as an intermetallic yttride; hafnium is completely in solid solution, and thus leads to a very fine distribution of small, internal oxide precipitates which then promote the branching growth of Al_2O_3 around them. There is also some evidence to suggest that enrichment of yttrium may occur in the internal oxide zone, promoting growth of larger particles. Figure 8, plate 1, compares the underside of the Al_2O_2 scales formed on Co–10Cr–11Al alloys containing either Y, Hf or HfO_2 additions.

Of course, the growth of pegs of the surface oxide into the alloy contributes to localized thickening of the scale, and thus in a sense there are two conflicting requirements. Low active element contents minimize thickening of the scale by inward growth around the internal oxide particles and prevent the formation of large oxide pegs, whereas higher active element contents are necessary to ensure sufficient pegs needed for efficient scale retention. Allam *et al.* (1978*a*) showed that a prior, controlled internal oxidation treatment in which the active element, hafnium, is converted to its oxide provides an excellent compromise. Internal oxidation reduces the hafnium content in the alloy, and forms a fine dispersion of HfO_2. This fine distribution results in a more uniform distribution of oxide pegs penetrating into the alloy which are more efficient in resisting scale spallation. Furthermore, the lower hafnium content in the matrix precludes further internal oxidation of hafnium during exposure, conditions which lead to solute enrichment, large HfO_2 precipitates and the formation of gross Al_2O_3 intrusions. Thus, by first internally oxidizing the alloy, the advantages of a high alloy active element content in producing sufficient pegs, but of the right size, coupled with minimal thickening of the surface scale, can be achieved.

PHILOSOPHICAL TRANSACTIONS OF THE ROYAL SOCIETY A MATHEMATICAL, PHYSICAL & ENGINEERING SCIENCES

7. Concluding remarks

The 'rare earth effect' has been seen, then, to be operative for a wide range of additions in an equally wide range of alloy systems, and at present there is no absolute indication of which type of additive is most effective, or at what concentration level. If the nucleation model is correct, and particles at the surface act as nucleation sites for all the oxide phases, producing a finer grained initial oxide film that can then achieve its steady state configuration more rapidly, then an oxide dispersion may be preferable to a reactive metal addition. The protective scale is more readily established in the early stages of oxidation and, if it is Cr_2O_3, can develop at lower alloy chromium contents: this may also be so for Al_2O_3 on aluminium-containing alloys, but the effect is marginal.

Reduction in the growth rate of the oxide seems virtually independent of the type of addition, but then in terms of oxidation resistance this is only a second order benefit. However, a reduced growth rate may also reduce growth stresses and minimize any depletion of the scale-forming element, chromium or aluminium, from the substrate. This could be of particular significance when the scale-forming element is in short supply, as for example in a protective coating.

Improvement in oxide scale adherence seems to be the major beneficial effect, and, of the mechanisms suggested, elimination of interfacial voids and peg formation seem to be of the most significance in most cases, but not necessarily in every case. For example, where there is only a very limited supply of the active metal addition, as in surface coatings or implanted ions, then peg formation is unlikely and chemical bonding is presumably more critical. Unless void formation is particularly critical during the early stages of oxidation, there is little to choose between reactive metal or oxide additions, and very low concentrations of additions seem sufficient. The formation of oxide pegs is perhaps the more decisive factor in oxide adhesion during the later stages of growth, whereas vacancy sink processes are important in the early stages. For both processes a fine, uniform distribution of small oxide pegs seem to be optimal. With metallic additions this is difficult to control, since essentially the active element oxidizes internally during high temperature exposure and these internally precipitated oxides form the nuclei around which the protective oxide forms the pegs. Clearly the distribution of internal oxides, and subsequently the pegs, depends on the exposure conditions and is thus not directly controllable. A pre-internal oxidation treatment is one, but not very practicable, way of controlling the oxide, and hence the peg, dispersion.

It appears that the composition of the dispersion is not critical. Nitrides can be used, but they are not as efficient as oxides. Carbides or even stable intermetallic compounds may be other possibilities since in general the following factors seem important:

(*a*) the dispersoid must be very stable so that it does not dissociate or dissolve in the matrix, and it is better if it does not oxidize;

(*b*) it is also better if the dispersoid does not contain the constituent that is going to form the protective scale; and

(*c*) it is possible to disperse the phase within the matrix in the right configuration.

The authors are grateful to Dr I. M. Allam for helpful discussions. They also acknowledge the Ministry of Defence for the support of experimental work in this field, and discussions with Dr A. Darling.

PHILOSOPHICAL TRANSACTIONS OF THE ROYAL SOCIETY A MATHEMATICAL, PHYSICAL & ENGINEERING SCIENCES

References (Whittle & Stringer)

Allam, I. A., Whittle, D. P. & Stringer, J. 1978*a* *Oxidat. Metals* **12**, 35–67.
Allam, I. A., Whittle, D. P. & Stringer, J. 1978*b* *Oxidat. Metals* **13**, 381–402.
Antill, J. E., Bennett, M. J., Carney, R. F. A., Dearnaley, G., Fern, F. H., Goode, P. H., Myatt, B. L., Turner, J. F. & Warburton, J. B. 1976 *Corros. Sci.* **16**, 729–745.
Antill, J. E. & Peakall, K. A. 1967 *J. Iron Steel Inst.* **205**, 1136–1142.
Beltran, A. M. 1970 *Cobalt* **46**, 3–14.
Davis, H. H., Graham, H. C. & Kvernes, I. A. 1971 *Oxidat. Metals* **3**, 431–451.
Felten, E. J. 1971 *J. electrochem. Soc.* **108**, 490–495.
Felten, E. J. 1976 *Oxidat. Metals* **10**, 23–28.
Fleetwood, M. J. 1966 *J. Inst. Metals* **94**, 218–223.
Flower, H. M. & Wilcox, B. A. 1977 *Corros. Sci.* **17**, 253–264.
Francis, J. M. & Jutson, J. A. 1968 *Corros. Sci.* **8**, 445–449.
Francis, J. M. & Whitlow, W. H. 1965 *Corros. Sci.* **5**, 701–710.
Francis, J. M. & Whitlow, W. H. 1966 *J. Iron Steel Inst.* **204**, 355–359.
Giggins, C. S. & Pettit, F. S. 1969 *Trans. metall. Soc. A.I.M.E.* **245**, 2509–2514.
Giggins, C. S. & Pettit, F. S. 1971 *Metall. Trans.* **2**, 1071–1078.
Giggins, C. S. & Pettit, F. S. 1975 *Wright Patterson Air Force Base, Contr.* no. F33615-72-C-1072.
Giggins, C. S., Kear, B. H., Pettit, F. S. & Tien, J. K. 1974 *Metall. Trans.* **5**, 1685–1688.
Golightly, F. A., Stott, F. H. & Wood, G. C. 1976 *Oxidat. Metals* **10**, 163–187.
Goncel, O. T., Stringer, J. & Whittle, D. P. 1978 *Corros. Sci.* **18**, 701–720.
Goncel, O. T., Whittle, D. P. & Stringer, J. 1979 *Corros. Sci.* **19**, 305–320.
Hagel, W. C. 1963 *Trans. Am. Soc. Metals* **56**, 583–594.
Hagel, W. C. & Seybolt, A. U. 1961 *J. electrochem. Soc.* **108**, 1146–1153.
Hauffe, K. & Block, J. 1951 *Z. phys. Chem.* **198**, 232–245.
Hollenberg, G. W. & Gordon, R. S. 1973 *J. Am. ceram. Soc.* **56**, 140–144.
Kofstad, P. & Hed, A. Z. 1970 *Werkstoffe Korros., Mannheim* **21**, 894–899.
Kuenzly, J. D. & Douglass, D. L. 1974 *Oxidat. Metals* **8**, 139–178.
Kumar, A., Hasrallah, M. & Douglass, D. L. 1974 *Oxidat. Metals* **8**, 227–263.
Kvernes, I. A. 1973 *Oxidat. Metals* **6**, 45–64.
Laurant, J. F. & Benard, J. 1958 *Physics Chem. Solids* **7**, 218–231.
Lees, D. G. & Calvert, J. 1976 *Corros. Sci.* **16**, 767–774.
Lewis, H. 1965 In *Proc. J. Int. d'Étude sur l'Oxidation des Métaux SERAI, Brussels.*
Lorenz, G. & Fischer, W. A. 1958 *Z. phys. Chem. neue Folge* **18**, 265–281.
Lowell, C. E. 1972 *Oxidat. Metals* **5**, 205–220.
Lowell, C. E., Deadmore, D. L., Grisafiffe, S. J. & Drell, I. L. 1971 *NASA tech. Note* no. NASA TN D-6290.
Lowell, C. E. & Sanders, W. A. 1972 *Oxidat. Metals* **5**, 221–239.
Lustmann, B. 1950 *Trans. metall. Soc. A.I.M.E.* **188**, 995–996.
McDonald, J. E. & Eberhart, J. G. 1965 *Trans. metall. Soc. A.I.M.E.* **233**, 512–517.
Michels, H. T. 1976 *Metall. Trans.* A **7**, 379–388.
Michels, H. T. 1977 *Metall. Trans.* A **8**, 273–278.
Nanni, P., Stoddart, C. T. H. & Hondros, E. D. 1976 *Mater. Chem.* **1**, 297–320.
Pfeiffer, H. 1957 *Werkstoffe Korros., Mannheim* **8**, 574–579.
Pfeil, L. B. 1937 *U.K. Patent* no. 459848.
Pfeil, L. B. 1945 *U.K. Patent* no. 574088.
Price, C. W., Wright, I. G. & Wallwork, G. R. 1973 *Metall. Trans.* **4**, 2423–2427.
Rhines, F. N. & Wulf, J. S. 1970 *Metall. Trans.* **1**, 1701–1708.
Ryabkina, M. M. & Rogel'berg, I. L. 1976 *Metallov. term. Obrab. Metall.* **7**, 11–15.
Seltzer, M. S. 1972 *Metall. Trans.* **3**, 3259–3264.
Seltzer, M. S. & Wilcox, B. A. 1972 *Metall. Trans.* **3**, 2357–2363.
Seltzer, M. S., Wilcox, B. A. & Stringer, J. 1972 *Metall. Trans.* **3**, 2391–2401.
Seybolt, A. U. 1966 *Corros. Sci.* **6**, 263–269.
Strafford, K. N. & Harrison, J. M. 1976 *Oxidat. Metals* **10**, 347–359.
Stringer, J. 1970 *Corros. Sci.* **10**, 513–543.
Stringer, J. 1972 *Oxidat. Metals* **5**, 49–58.
Stringer, J. & Hed, A. Z. 1971 *Oxidat. Metals* **3**, 571–576.
Stringer, J. & Wright, I. G. 1972 *Oxidat. Metals* **5**, 59–84.
Stringer, J., Allam, I. M. & Whittle, D. P. 1977 *Thin solid Films* **45**, 377–384.
Stringer, J., Hed, A. Z., Wallwork, G. R. & Wilcox, B. A. 1972*a* *Corros. Sci.* **12**, 625–636.
Stringer, J., Wilcox, B. A. & Jaffee, R. I. 1972*b* *Oxidat. Metals* **5**, 11–36.
Tallman, R. L. & Gulbransen, E. A. 1968 *Nature, Lond.* **218**, 1046–1047.

PHILOSOPHICAL TRANSACTIONS OF THE ROYAL SOCIETY A MATHEMATICAL, PHYSICAL & ENGINEERING SCIENCES

Tedmon, Jr., C. S. 1966 *J. electrochem. Soc.* **113**, 766–772.
Tien, J. K. & Pettit, F. S. 1972 *Metall. Trans.* **3**, 1587–1599.
Wallwork, G. R. & Hed, A. Z. 1971 *Oxidat. Metals* **3**, 229–241.
Whittle, D. P., El Dahshan, M. E. & Stringer, J. 1977 *Corros. Sci.* **17**, 879–891.
Whittle, D. P. & Wood, G. C. 1968 *Inst. J. Metals* **96**, 115–123.
Wood, G. C. 1971 *Werkstoffe Korros., Mannheim* **22**, 491–503.
Wood, G. C. & Boustead, J. 1968 *Corros. Sci.* **8**, 719–723.
Wright, I. G. & Seltzer, M. S. 1973 *Metall. Trans.* **4**, 411–417.
Wright, I. G. & Wilcox, B. A. 1974 *Oxidat. Metals* **8**, 283–301.
Wright, I. G., Wilcox, B. A. & Jaffee, R. I. 1975 *Oxidat. Metals* **9**, 275–305.
Wukusick, C. S. & Collins, J. F. 1964 *Mater. Res. Stand.* **4**, 637–646.

PHILOSOPHICAL TRANSACTIONS OF THE ROYAL SOCIETY A MATHEMATICAL, PHYSICAL & ENGINEERING SCIENCES

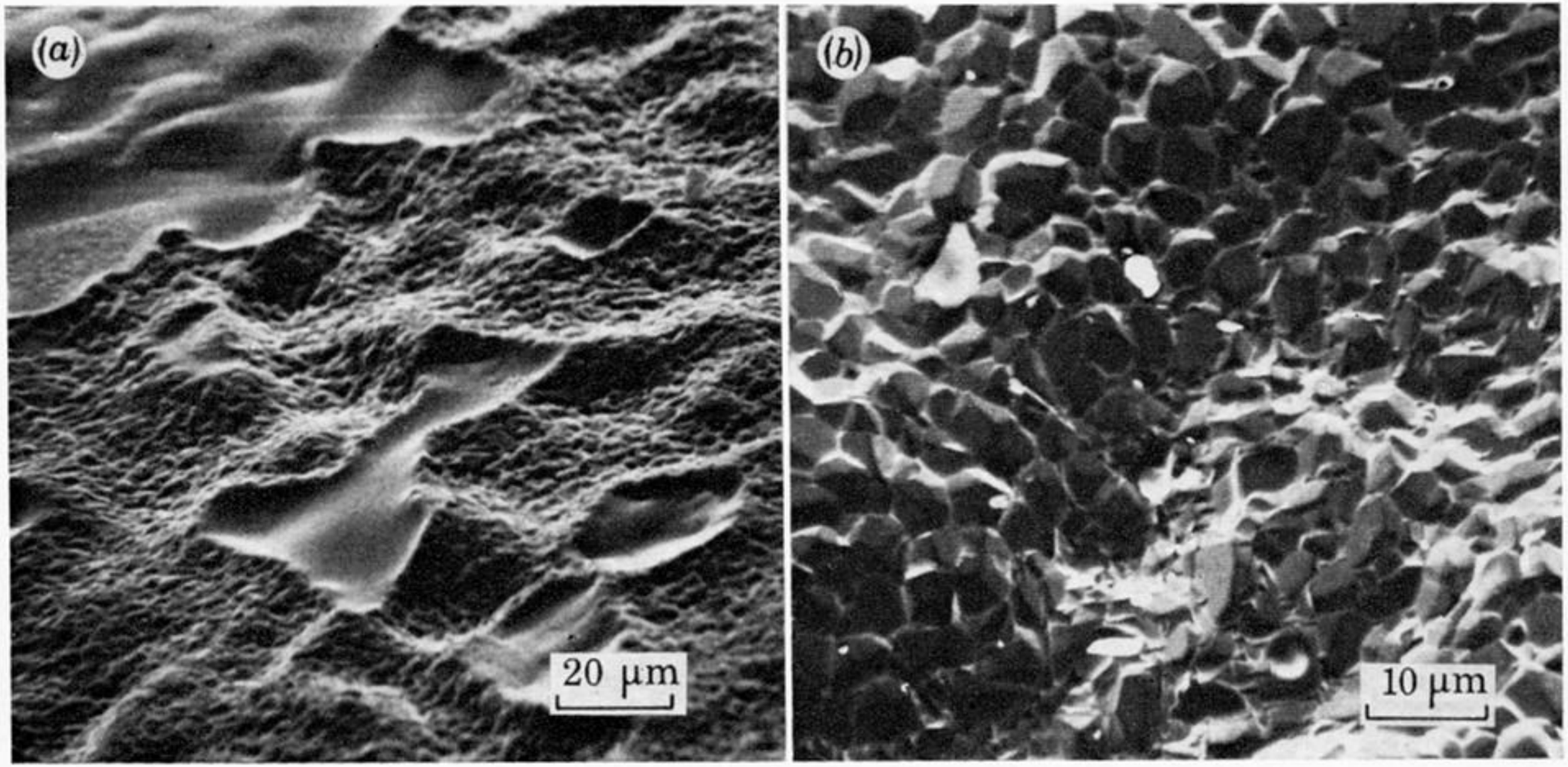

FIGURE 4. The alloy surface after removal of the scale of a specimen of (*a*) Co–15Cr–8Al oxidized for 190 h at 1200 °C and (*b*) Co–10Cr–11Al–0.1Y oxidized for 1000 h at 1200 °C. The surface of the Y-containing alloy is completely imprinted with oxide grains; that of the Y-free alloy contains smooth, imprint-free regions where the scale was not in contact with the alloy. (Allam *et al.* 1978*a*.)

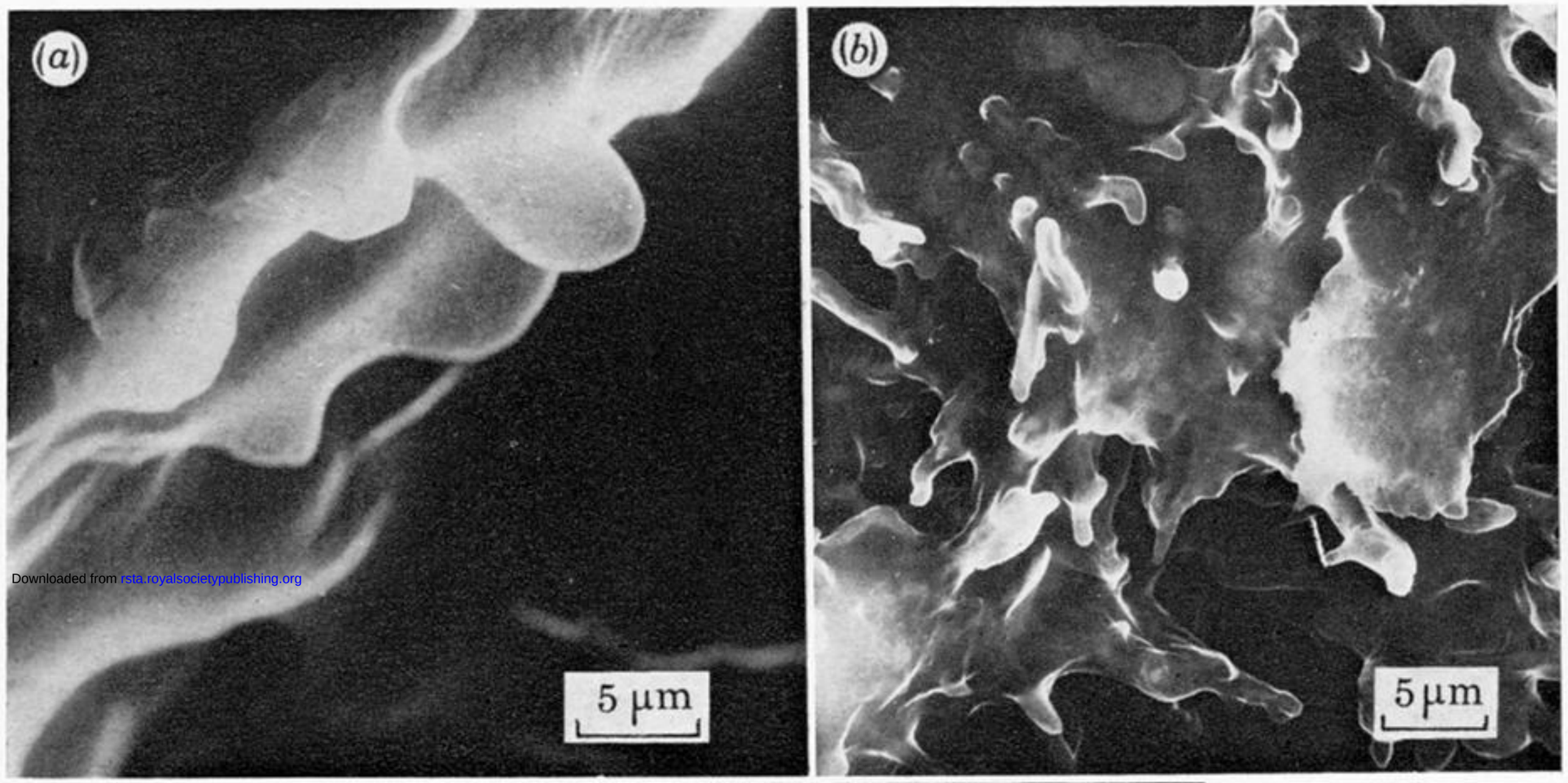

FIGURE 8. A comparison of the underside of the Al_2O_3 scale, stripped from the alloy. (*a*) Co–10Cr–11Al–0.3Y oxidized for 75 h at 1200 °C. (*b*) Co–10Cr–11Al–1Hf oxidized for 75 h at 1200 °C. (*c*) Co–10Cr–11Al–1Hf, internally oxidized in a CoAl–Al_2O_3 mixture for 200 h at 1200° C to convert the Hf into an oxide dispersion, and then oxidized for 75 h at 1200 °C. (Allam *et al.* 1978*b*.)

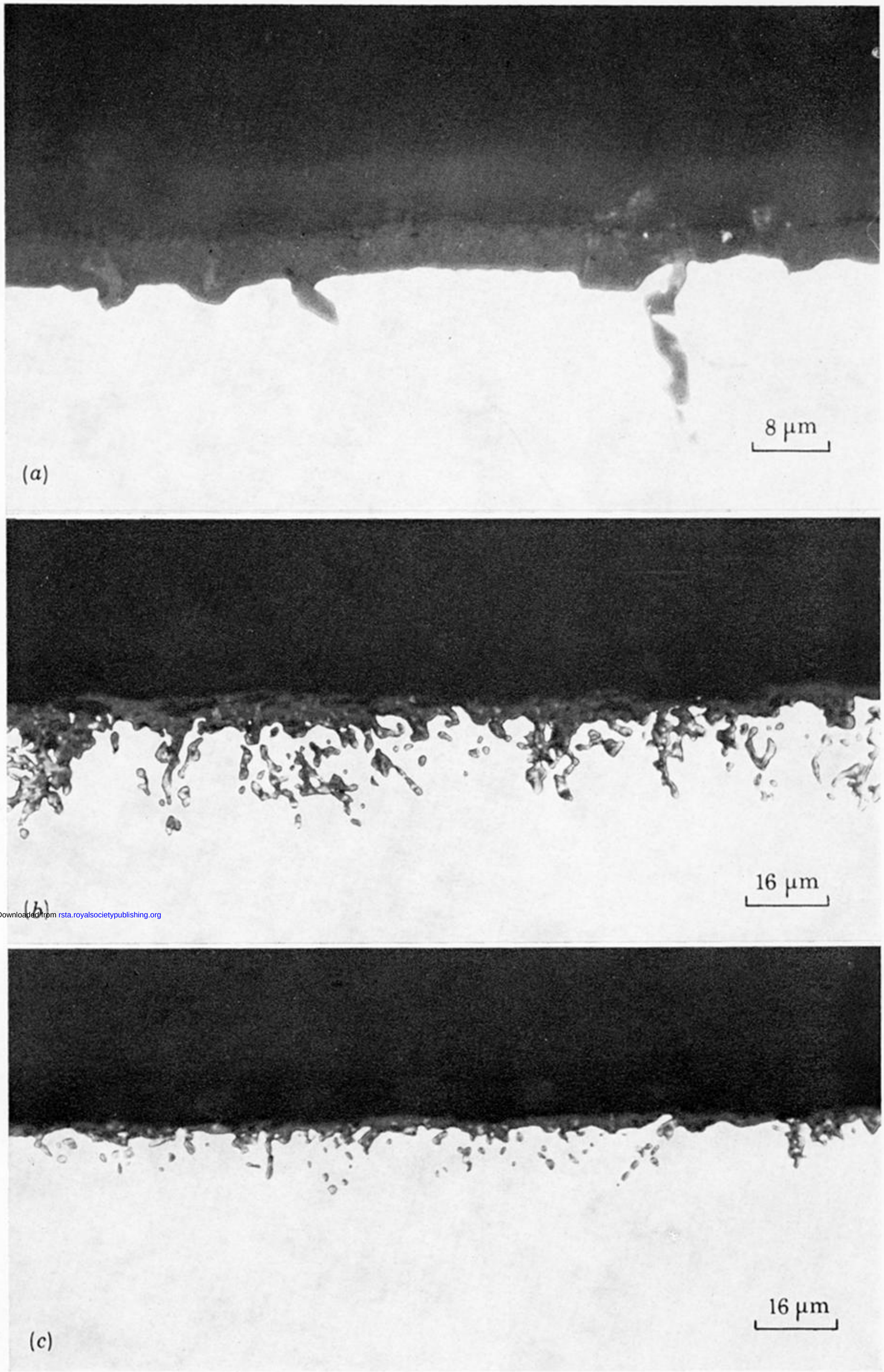

FIGURE 5. A comparison of the morphology of oxide peg development: (*a*) Co–10Cr–11Al–1Y oxidized for 1000 h at 1200 °C; (*b*) Co–10Cr–11Al–1Hf oxidized for 350 h at 1200 °C; (*c*) Co–10Cr–11Al–1Hf internally oxidized in a CoAl–Al_2O_3 mixture for 200 h at 1200 °C to convert the Hf into an oxide dispersion, and then oxidized for 350 h at 1200 °C.

The intrusions in the Y-containing alloy are relatively large and infrequent along the interface. In comparison, the Hf-containing alloy contains profuse intrusions which can grow quite large, while the HfO_2-containing alloy has a finer, more regular distribution. (Allam *et al.* 1978*b*.)